



HHS Public Access

Author manuscript

Biomacromolecules. Author manuscript; available in PMC 2022 November 08.

Published in final edited form as:

Biomacromolecules. 2021 November 08; 22(11): 4489–4500. doi:10.1021/acs.biomac.1c00719.

Correlation of Bulk Degradation and Molecular Release from Enzymatically Degradable Polymeric Hydrogels

Nan Wu, Kelly M. Schultz

Department of Chemical and Biomolecular Engineering, Lehigh University, Bethlehem, Pennsylvania 18015, United States

Abstract

In this work, we establish a quantitative correlation between molecular release and material degradation. We characterize a radical-initiated photopolymerized hydrogel and base-initiated Michael addition-polymerized hydrogel, which form gels through distinct crosslinking reactions. Both scaffolds use the same degradable peptide crosslinker, which enables them to be degraded through the same enzymatic degradation reaction. A fluorescently labeled poly(ethylene glycol) molecule is chemically conjugated into the scaffold and is released during enzymatic degradation. Real-time changes in scaffold rheological properties during degradation are measured using bulk rheology. Molecular release is measured by quantifying the change in fluorescence in the incubation liquid and the hydrogel scaffold. A complicating factor, previously described in the literature, is that shear may cause increased crosslinking, resulting in an increase in the storage modulus after initiation of degradation, which changes release profiles by limiting the initial release of molecules. Therefore, we also test the hypothesis that shear induces additional crosslinking in degrading hydrogel scaffolds. To determine whether shear changes rheological properties during scaffold degradation, enzymatic degradation is characterized using bulk rheology as materials undergo continuous or minimal shear. To determine the effect of shear on molecular release, shear is induced by shaking the material during incubation. Release is characterized from scaffolds that are incubated with continuous or without shaking. We determine that shear does not make a difference in scaffold degradation or release regardless of the gelation reaction. Instead, we determine that the type of hydrogel crosslinking reaction greatly affects both material degradation and molecular release. A hydrogel crosslinking by base-initiated Michael addition does undergo further crosslinking at the start of degradation. We correlate release with enzymatic degradation for both scaffolds. We determine that the material storage modulus is indirectly correlated with release during degradation. These results indicate that rheological characterization is a useful tool to characterize and predict the release of molecules from degrading hydrogels.

Corresponding Author Kelly M. Schultz – Department of Chemical and Biomolecular Engineering, Lehigh University, Bethlehem, Pennsylvania 18015, United States; Phone: (610) 758-2012; kes513@lehigh.edu; Fax: (610) 758-5057.

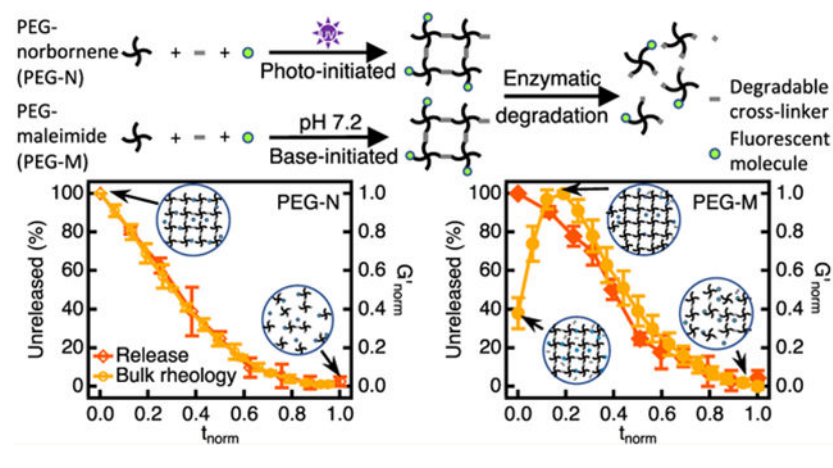
Supporting Information

The Supporting Information is available free of charge at <https://pubs.acs.org/doi/10.1021/acs.biomac.1c00719>.

Rheology of starting materials: unswollen moduli of both polymer-peptide hydrogels, swollen moduli of both scaffolds with and without PEG-fluorescein, calibration curves used to calculate PEG-fluorescein concentration and cumulative mass release percentage: first batch of PEG-fluorescein and second batch of PEG-fluorescein, molecular release from PEG-norbornene hydrogels under shear, correlation of release with degradation under minimal shear, and Korsmeyer-Peppas-Ritger model fitting: PEG-norbornene hydrogels and PEG-maleimide hydrogels (PDF)

The authors declare no competing financial interest.

Graphical Abstract



INTRODUCTION

Novel materials, including biodegradable hydrogels, have been developed and extensively characterized for their use as vehicles for targeted, controlled drug delivery. Drug delivery is not a simple process and is affected by many factors including the physicochemical properties of the drug molecules, the release environment, and the structural characteristics of the hydrogel.¹⁻³ Hydrogel characteristics of particular interest are the kinetics and change in the scaffold structure during degradation, which results in molecular release. Extensive work has been focused on how to tune the degradation of delivery systems by tailoring material composition or environmental conditions for particular applications.⁴⁻⁹ However, scaffold degradation is generally characterized with swelling or mass loss data. These experiments can be inaccurate due to the complication of having inconsistent amounts of water in the scaffold for each measurement.^{4,7,10,11} Recently, techniques to precisely measure the evolving rheology of the material during degradation have been developed. These techniques include microrheology,¹²⁻¹⁶ bulk rheology,¹⁷⁻²⁰ a combination of microrheology and bulk rheology,²¹ and μ^2 rheology (the combination of microrheology and microfluidics).^{22,23} In this work, we covalently tether fluorescently labeled molecules to a hydrogel network and characterize matrix degradation using bulk rheology. We also quantify the corresponding release profile by measuring the change in fluorescence in the scaffold and incubation liquid. Our work provides a technique that enables a quantitative correlation between degradation and molecular release to be built.

For delivery vehicles, scaffolds are designed with tunable degradability to enable release of molecules. This has resulted in extensive studies that have focused on tuning degradation by varying the scaffold formulation and responsiveness to environmental cues. Work on tuning degradability with the scaffold formulation has focused on changing the polymer concentration, polymer molecular weight, and functionality of molecules.⁵⁻⁷ Inducing and tuning degradation through scaffold responsiveness to environmental conditions have focused on cues such as incubation pH,^{23,24} enzymes in the fluid environment,^{5,25} and adding ultrasound.^{26,27} These approaches have also been used to tune molecular release by changing material properties or stimuli for each application to customize release

profiles.^{1,28-34} Varying these parameters requires trial and error experiments and can be timeconsuming and expensive. Therefore, establishing a correlation between material rheology and molecular release can enable efficient design of a controlled, targeted delivery vehicle, especially from new materials.

Our work aims to fill this gap and quantitatively correlate material rheology and molecular release. Rheology precisely measures the evolution of scaffold stiffness during degradation. Few studies have linked changes in rheology during degradation to drug release behavior.^{19,35} Previous work measures the effect of enzyme concentration on both bulk rheological degradation and protein release; however, this work does not provide a direct relation between release and degradation kinetics.¹⁹ A correlation between material rheology and molecular release would enable quantitative predictions of release from measurements of material degradation. Other studies have correlated molecular release mechanisms in nondegradable matrices using mathematical models.^{2,36-38} Due to the complexity of degrading scaffolds, it has been difficult, at best, to extend these models to degradable materials.² Instead, these mathematical models assume that the scaffold is at equilibrium and a drug is released by the most significant driving force (e.g., drug molecule diffusion or hydrogel swelling).² Therefore, model predictions and experimental data do not always agree, which means that the existing mathematical models may not fully explain the molecular release mechanism. This is especially difficult in stimuli-triggered delivery systems where several processes occur simultaneously, resulting in molecular release. These processes include matrix degradation, drug molecule diffusion within porous media, and hydrogel swelling. To better understand the release mechanism and predict release performance, it is critical to quantitatively correlate material degradation and molecular release.

To establish a correlation between molecular release and hydrogel degradation, we use enzymatically degradable well-defined poly(ethylene glycol) (PEG)-peptide hydrogels. We begin with well-defined systems to focus on developing a quantitative correlation that will inform the design of future advanced drug delivery materials using rheology. Enzymatically degradable polymeric matrices are made using two types of step-growth reactions: a radical-initiated thiol:ene reaction and a base-initiated thiol:maleimide reaction. The backbones of these scaffolds are multi-arm star PEG molecules with distinct end-functional groups. These PEG molecules are crosslinked with the same enzymatically degradable peptide sequence, enabling them to be degraded by the same reaction. The radical-initiated hydrogel is photopolymerized and uses thiol:ene click chemistry. These scaffolds consist of 4-arm star PEG molecules end-functionalized with norbornene, which chemically crosslink with matrix metalloproteinase (MMP)-degradable peptides.^{12,39-41} Base-initiated polymerized hydrogels use thiol:maleimide chemistry to form covalent bonds. The 4-arm star PEG-maleimide crosslinks with the same MMP-degradable peptide by step-growth polymerization after mixing.⁴²⁻⁴⁵ In both scaffolds, PEG-fluorescein is chosen as a model drug molecule. This molecule has one end functionalized with thiol. This enables the fluorescent molecule to covalently tether to a free functional group on the polymer backbone during either radical-initiated or base-initiated crosslinking. These scaffolds are degraded at the MMP-degradable peptide crosslinker by incubation in collagenase, which is a mixture of enzymes including MMPs. During degradation, fluorescent molecules are released.

PEG–fluorescein is chosen as our model cargo due to several characteristics of fluorescein and PEG that make it ideal for this application. Fluorescein and its derivatives are commonly used as model therapeutics in drug delivery systems, such as colloid liquid crystals,⁴⁶ microcapsules,⁴⁷ silica nanocapsules,⁴⁸ hybrid materials,⁴⁹ and stimuli-responsive hydrogels.^{1,50,51} Fluorescein is chosen as a model drug because its features are similar to those of many traditional therapeutics including hydrophobicity, charge, size, and the chemical structure.^{47,49-51} In addition, the strong fluorescence from fluorescein makes this molecule sensitive enough to be detected and precisely measured using fluorescence spectroscopy and many other fluorescence-reading devices.⁴⁷ PEG is chosen because of its versatile molecular weight, which enables PEG to mimic the size of various therapeutics from small-molecule drugs to large biomacromolecules. PEG is also easily functionalized by a wide range of chemistries, enabling PEG to be tethered to a hydrogel scaffold.^{1,43,52} We would like to emphasize that we begin with idealized hydrogel scaffolds, and PEG–fluorescein is used as a model cargo to develop techniques and correlations between rheology and molecular release.

We also investigate the role of shear and crosslinking reaction in the relationship between molecular release and rheology during scaffold degradation. Shear induced during material processing or characterization could greatly affect the material structure and change material properties.^{18,22,42,53} Previous work used small amplitude oscillatory shear to measure degradation kinetics and rheology of an enzymatically degradable hydrogel. An increase in the modulus was measured after incubating the material in a bath of enzymes, which should result in material degradation or a decrease in the modulus.¹⁸ We test two hypotheses to explain this: (1) shear induces additional crosslinking or changes in the structure, such as alignment, during incubation or (2) during swelling, additional crosslinks can form. Oscillatory shear could create an aligned structure or increase functional group mobility to crosslinks further causing an increase in the modulus. Additionally, a system that crosslinks upon mixing could also allow the material to continue to gel during swelling, since the reaction can continuously occur and functional groups can become available for crosslinking as the structure swells. We first investigate the effect of shear and crosslinking reaction on scaffold degradation and release, prior to determining a quantitative correlation between these processes.

In this work, we measure enzymatic degradation of both radical-initiated and base-initiated biodegradable hydrogels. We measure the rheological evolution of these scaffolds using bulk rheology. Release of our covalently tethered fluorescent molecule is measured by changes in the fluorescence of the incubation media and gel. To determine whether shear changes scaffold degradation and molecular release, these scaffolds are measured using either continuous or minimal shear during bulk rheological characterization and molecular release experiments. These measurements confirm that shear does not affect scaffold degradation or molecular release regardless of the crosslinking reaction. We do find that changing the type of crosslinking reaction does change degradation and molecular release. The release from degrading radical-initiated photopolymerized hydrogels has zero-order kinetics, indicating that molecular release results from enzymatic degradation. The release from base-initiated polymerized hydrogels proceeds in two steps: minimal release during additional crosslinking after incubation and accelerated release during enzymatic degradation. We also

quantitatively correlate release with scaffold degradation. There is an indirect relationship between molecular release and the storage modulus during scaffold degradation.

MATERIALS AND METHODS

Gel Fabrication.

Two hydrogel scaffolds are characterized in this work: (1) a radical-initiated photopolymerized PEG–norbornene scaffold and (2) a base-initiated polymerized PEG–maleimide scaffold. The photopolymerized hydrogel consists of 4-arm star PEG end-functionalized with norbornene ($M_n = 20,000 \text{ g mol}^{-1}$, $f = 4$ where f is the functionality, 3 mM, JemKem Technology) that chemically crosslinks with a biscysteine containing MMP-degradable peptide sequence (KCGPQG↓IWGQCK where ↓ is the cleavage site, $M_n = 1305 \text{ g mol}^{-1}$, $f = 2$, 7.2 mM, Bachem). The thiol in the cysteine reacts with an –ene group on the PEG by thiol:ene step-growth photopolymerization. All photopolymerized hydrogels are made at a thiol:ene ratio of 0.65. Lithium phenyl-2,4,6-trimethylbenzoylphosphinate (LAP, 1.7 mM) is the photoinitiator. LAP is synthesized using previously published protocols.⁵⁴ The hydrogel precursor solution is a mixture of PEG–norbornene, MMP-degradable peptide crosslinker, LAP, and 1× phosphate buffered saline (PBS) (Fisher Scientific, pH 7.2). The mixed polymer precursor is pipetted into a cylindrical polydimethylsiloxane (PDMS, Dow Corning) sample chamber, and photopolymerization occurs when the hydrogel precursor solution is exposed to UV light (6 mW/cm^2 , 365 nm, collimated UV lamp, Analytik Jena US) for 3 min. The PDMS chamber is described below.

The base-initiated hydrogel is composed of 4-arm star PEG–maleimide ($M_n = 20,000 \text{ g mol}^{-1}$, $f = 4$, 3 mM, Jenkem Technology), which chemically crosslinks with the same MMP-degradable peptide (KCGPQG↓IWGQCK, $M_n = 1305 \text{ g mol}^{-1}$, $f = 2$, 3.9 mM, Bachem) described above. The thiol group in the cysteine covalently crosslinks with a maleimide by Michael addition via step-growth polymerization. In our system, we use a thiol:maleimide ratio of 1.2. Polymers are mixed in 1× PBS (Fisher Scientific, pH 7.2) to the specified concentrations. The gelation reaction spontaneously occurs by mixing PEG–maleimide and the MMP-degradable peptide crosslinker.

The gelation reaction for thiol:maleimide can be relatively fast at pH 7.2, which could lead to a heterogeneous network. This reaction can be slowed by crosslinking the PEG–maleimide with a negatively charged peptide (i.e., a peptide such as our crosslinker that contains thiol in the amino acid cysteine). This will result in a more uniform hydrogel network in comparison to gelation at a lower pH or decreased polymer concentration.⁴³ Wehrman et al. also measured heterogeneity of a similar thiol:maleimide hydrogel during the gelation reaction.⁴² This work uses 4-arm PEG–maleimide ($M_n = 20,000 \text{ g mol}^{-1}$, $f = 4$) crosslinked with PEG–dithiol ($M_n = 1500 \text{ g mol}^{-1}$, $f = 2$) through step-growth polymerization, which would be a faster reaction and could result in a heterogeneous network. The non-Gaussian parameter, α_{NG} , is calculated from multiple particle tracking microrheology data. This value indicates structural heterogeneity. When the polymer concentration is 3 wt % PEG–maleimide, which is a value below the concentration used in this work (6 wt %) and below the overlap concentration, they determined that as gelation proceeds, α_{NG} is less than 0.1. This indicates that the network is homogeneous

throughout the gelation reaction. In addition, α_{NG} does not increase post-gelation, indicating formation of a homogeneous crosslinked structure. They also measured the same scaffold at a concentration above the one used in this work, 10 wt % PEG–maleimide. They measured values of α_{NG} that are slightly higher, with a maximum value of 0.25. These values are still very low and indicate that the structure is relatively homogeneous. Therefore, these previous studies indicate that the structure of our material should be relatively homogeneous.

Once the solution is well mixed, the precursor solution is transferred to a PDMS sample chamber (Dow Corning), and samples are kept in a humidified environment. We equilibrate the PEG–maleimide hydrogels for 3.5 h to ensure that the gelation reaction proceeds to completion. The composition of the material is chosen to ensure that the unswollen moduli of this scaffold are the same as the unswollen PEG–norbornene hydrogel moduli. This is determined using bulk rheology and indicates that both scaffolds have a similar crosslink density at the start of each experiment. A frequency sweep of the two materials is shown in Figure S1 in the Supporting Information.

All PEG–maleimide samples are equilibrated in a humidified environment to allow the crosslinking reaction to proceed while also preventing the gel from drying out. The humidified environment is created using a large Petri dish (150 × 15 mm, Corning Falcon) filled with 1× PBS. To prevent sample contact with the PBS, PDMS sample chambers are placed on a piece of transparency (8.5 × 11 in, Apollo), which is separated from the bottom of the Petri dish using spacers. During gel equilibrium, the Petri dish is sealed with Parafilm (Fisher Scientific) to prevent evaporation.

All hydrogels are made in cylindrical PDMS sample chambers. PDMS is made by mixing a curing agent and silicone elastomer base at a ratio of 1:10 (PDMS, Dow Corning). The mixed PDMS is gently poured into a Petri dish (150 × 15 mm, Corning Falcon) and cured at 65°C overnight. These chambers are made by cutting a ring from a flat sheet of cured PDMS with an 8 mm inner diameter and 10 mm outer diameter using biopsy punches (Integra Biosciences). The PDMS ring is attached to a clean transparency using UV-curable thiol:ene glue (NOA 81, Norland Products INC). The device is exposed to UV light (6 mW/cm², 365 nm, Analytik Jena US) for approximately 1 min, which bonds the PDMS ring to the transparency, completing the sample chamber. The gels are then polymerized in the sample chamber as described above. After hydrogel fabrication, the PDMS ring is carefully removed, and hydrogels are ready for bulk rheological measurements.

Preparation of Collagenase.

Hydrogel degradation and molecular release are initiated by incubating scaffolds in collagenase solution. A total of 1 mg mL⁻¹ collagenase solution is made with collagenase from *Clostridium histolyticum* (Sigma-Aldrich, activity 125 CDU/mg solid, 0.25–1.0 FALGPA units/mg solid) powder dissolved in 1× PBS (Fisher Scientific, pH 7.2). The concentration of 1 mg mL⁻¹ collagenase is chosen to ensure that enough data can be collected of these dynamic processes without the experiment taking an excessive amount of time. This concentration of collagenase is used for bulk rheological characterization, dynamic molecular release, and gel size measurements for both types of hydrogels.

Rheological Characterization of Hydrogel Degradation.

100 μL gels are made as described above with 8 mm diameters in PDMS sample chambers. After gel fabrication, the sample chamber PDMS ring is removed, and the hydrogel sample is immediately transferred onto the Peltier plate of the rheometer. A strain-controlled AR-G2 rheometer (TA Instruments) with sandblasted 8 mm parallel plate geometry is used for all measurements. All rheological measurements are taken from three replicates of each type of hydrogel, and the storage moduli are reported as the average of these measurements with the standard deviation reported as the error bars.

For bulk rheological measurements that impart continuous shear, the evolution of material rheological properties is measured using a time sweep as the gel is soaked in 6 mL of 1 mg mL^{-1} collagenase in an immersion cup (TA Instruments). Oscillatory shear is continuously applied at 1 Hz in the linear viscoelastic regime under constant 1% strain. Degradation kinetics are measured by the storage, G' , and loss modulus, G'' , as a function of time. To measure the equilibrium moduli at specified time intervals during the degradation reaction, a frequency sweep in the linear viscoelastic regime from 0.1 to 10 Hz is done at 1% strain every 10 minutes during the time sweep.

To measure hydrogel rheological properties under minimal shear, bulk rheological characterization is done on discrete hydrogel samples. A total of 10 separate hydrogel samples of 100 μL are made using the protocol described in the Gel Fabrication section. After gel fabrication, each gel is gently moved to different wells in a 12-well plate (127.63 \times 85.47 \times 20.19 mm, Corning Falcon). After gels are in the wells, each well is filled with 700 μL of 1 mg mL^{-1} collagenase to incubate and degrade the samples. This amount of collagenase contacts the sides of the hydrogel but does not cover the top surface, which mimics the *in situ* measurement conditions on the rheometer. Each hydrogel sample has a different incubation time from 30 to 240 min in 30 min increments. For example, one hydrogel will be incubated for 30 min and then measured. A second hydrogel will be incubated for 60 min and then measured. Each hydrogel is incubated for a given time and measured only once. The equilibrium modulus of different samples is measured with a frequency sweep at 1% strain from 0.1 to 20 Hz. Samples at 0 min degradation are immediately measured without collagenase incubation.

Tethering Fluorescent Molecules to the Scaffold and Release Studies.

PEG–fluorescein end-functionalized with thiol ($M_n = 1,000 \text{ g mol}^{-1}$, $f = 1$, Nanocs Inc.) is used as a model cargo for release studies. We chose 1 kDa PEG–fluorescein to mimic the size of small-molecule drugs.

Each set of release experiments is carried out on three hydrogels with PEG–fluorescein and one control hydrogel without PEG–fluorescein. PEG–fluorescein is covalently tethered to each hydrogel during gel fabrication. PEG–fluorescein-loaded PEG–norbornene hydrogels are fabricated by adding PEG–fluorescein prior to the thiol:ene crosslinking reaction. A total of 10 μL of the polymer precursor solution with a final concentration of 0.49 mM PEG–fluorescein is pipetted into a well in a 96-well plate (127.76 \times 85.59 \times 14.30 mm, Fisher Scientific). The mixed precursor is exposed to UV for 3 min (6 mW/cm^2 , 365 nm, Analytik

Jena US) to gel the scaffold. Similarly, to fabricate PEG–fluorescein-loaded PEG–maleimide hydrogels, PEG–fluorescein is mixed into the PEG–maleimide precursor solution described earlier at a final concentration of 0.72 mM. A total of 10 μL of the polymer precursor solution is pipetted into a well in a 96-well plate ($127.76 \times 85.59 \times 14.30$ mm, Fisher Scientific) and equilibrated for 3.5 h to enable complete gelation. To prevent evaporation, $1\times$ PBS is added to the gaps between the wells, and the plate is covered and sealed with Parafilm.

The ratio of thiol groups in the PEG–fluorescein to thiol groups in the MMP-degradable crosslinker is 1:20 in both hydrogels. This low concentration of PEG–fluorescein is chosen to ensure that covalently tethering this model cargo into the hydrogel during crosslinking will not affect the storage moduli or crosslink density of the scaffold. We determine that tethering PEG–fluorescein to the network does not change the scaffold structure or properties. This is done by measuring the swollen modulus and confirming that it does not change. Results of these measurements are shown in Figures S2 and S3 in the Supporting Information. PEG–fluorescein-loaded hydrogels are rinsed three times with 200 μL of $1\times$ PBS to remove any untethered fluorescent molecules from the scaffold.

Prior to release studies, a calibration curve is made to calculate the concentration of PEG–fluorescein from measurements of fluorescence intensity. This is done by diluting PEG–fluorescein to known concentrations and measuring the resulting fluorescence intensity using a fluorescence imager (Amersham Biosciences, Typhoon Imager model 5). The fluorescein intensity is read at a laser wavelength of 488 nm with a Cy2 filter at 525 ± 20 nm. All calibration curves are provided in Figures S4 and S5 in the Supporting Information.

During our experiments, 10 μL PEG–fluorescein-loaded hydrogels are incubated in 200 μL of 1 mg mL^{-1} collagenase in a 96-well plate. Molecular release from the hydrogel to the surrounding collagenase solution is defined as the sol-sample. The fluorescence intensity of a sol-sample is measured and used to calculate the release profile. A total of 20 μL of the sol-sample is taken from the hydrogel incubation fluid every 20 min and replaced with 20 μL of fresh 1 mg mL^{-1} collagenase solution to maintain the incubation environment. This 20 μL sol-sample is put in a separate 96-well plate and diluted $10\times$ in the same concentration of collagenase before fluorescence is read. Fluorescence intensity of the sol-sample is measured using a fluorescence imager (Amersham Biosciences, Typhoon Imager model 5) at a laser wavelength of 488 nm with a Cy2 filter at 525 ± 20 nm to determine the amount of fluorescein released into the well. Fluorescein concentration at each time point is calculated using the appropriate calibration curve. Once the concentration in the sol-sample is determined, it is used to calculate the cumulative mass released at time t , M_t , using

$$M_t = C_t V + \sum C_{t-1} V_s \quad (1)$$

where C_t is the concentration of fluorescein measured at time t , V is the total volume of incubation media, which is 200 μL , and V_s is the volume of the sol-sample, which is 20 μL .^{33,55} The release percentage is then calculated using

$$\text{Release \%} = \frac{M_t}{M_\infty} \times 100 \% \quad (2)$$

where M_∞ is the total weight of molecules released throughout the experiment.^{30,33,56} All experiments measuring molecular release are done in triplicate.

To determine how shear influences molecular release in both hydrogel scaffolds, gels are incubated in collagenase on a shaker (Thermo Fisher Scientific) at a controlled frequency of 70 rpm, which is equivalent to 1.16 Hz.⁵⁷ This incubation condition is referred to as shake release. Samples are also incubated without shaking, which is a minimal-shear condition and is referred to as nonshake release. In shake release, we constantly shake the material to induce shear and continuously measure material properties. The shaking conditions chosen are similar to the shear imparted during the time sweep measured with bulk rheology. In nonshake release, minimal shear is exerted on the material, and we measure material properties. These conditions mimic a single frequency sweep after incubation of the gel with bulk rheology.

Characterization of Gel Volume during Release.

We measure the change in volume of these hydrogels during the degradation reaction. Each set of experiments contains two samples without PEG–fluorescein and one sample that includes PEG–fluorescein. A 70 μL hydrogel sample is made in a 6 mm diameter PDMS sample chamber using the same protocols described in the Gel Fabrication section. Once fabricated, samples are moved to separate wells in a 12-well plate and incubated in 2100 μL of 1 mg mL^{-1} collagenase. This amount of collagenase completely submerges the hydrogel samples. The diameter and height of each sample are measured every 20 min with a micrometer (FunOwlet US) until the gel is fully dissolved. Data are reported as the average volume with error bars that are the standard deviation from the three replicates. To make these studies parallel with the bulk rheology and release measurements, the change in gel size is also measured in samples that are incubated during constant shaking or without shaking using the same conditions outlined for the release studies.

RESULTS AND DISCUSSION

In this work, two types of enzymatically degradable hydrogels are characterized to establish a quantitative correlation between material rheology and molecular release. We determine the role of the crosslinking mechanism by measuring rheology and molecular release from materials with different crosslinking reactions. We also establish whether shear imposed on the hydrogels during degradation changes rheological property evolution and molecular release. This study enables quantitative predictions of molecular release from material rheological properties, which in turn, advance material design and engineering of a controlled, targeted drug delivery vehicle.

We measure dynamic molecular release of a model cargo covalently tethered to the scaffold and bulk rheological evolution during enzymatic degradation. The scaffolds that are characterized have different crosslinking chemistries: (1) a radical-initiated thiol:ene

chemistry and (2) a base-initiated thiol:maleimide chemistry. These two types of hydrogels undergo step-growth polymerization reactions and are both degraded by the same enzymatic degradation reaction. Due to the difference in the gelation reaction, the effect of the gelation mechanism on scaffold degradation or molecular release will be investigated.

The effect of shear imparted on the material is also investigated in this work. Of particular interest is a phenomenon reported in the literature—the modulus increases at the beginning of degradation in an enzyme-catalyzed disulfide crosslinked hydrogel and then decreases until reaching a degraded plateau value.¹⁸ In this work, they hypothesize that the increase in the modulus is possibly due to oscillatory shear used to collect rheological measurements changing the scaffold material properties by potentially creating new structures and enabling further crosslinking of the material. We also hypothesize that the type of gelation reaction could promote a scaffold to crosslink more or change the material structure once it is incubated. For a base-initiated thiol:maleimide crosslinking hydrogel, the crosslinks react once they find the complimentary chemistry, which could occur as molecular motion becomes less restricted when the scaffold swells. For a radical-initiated thiol:ene crosslinking hydrogel, only shear could cause a change in the structure of the material, potentially inducing alignment, which could increase the material modulus. To explain this phenomenon, we investigate whether shear or the type of crosslinking reaction is the source of the measured increase in the modulus after incubation.

To determine the roles of the gelation reaction and shear in scaffold degradation, we characterize enzymatic degradation of both radical-initiated and base-initiated crosslinking hydrogels. Bulk rheological characterization imparts either continuous shear (defined as continuous bulk measurements) or minimal shear (defined as discontinuous bulk measurements). A continuous bulk measurement is a time sweep of a single sample throughout the entire degradation reaction. A discontinuous bulk measurement is a single frequency sweep on multiple identical samples, each with different incubation times in the enzyme solution. All samples are degraded with 1 mg mL⁻¹ collagenase.

Results from our work will be discussed by first addressing whether shear changes scaffold degradation and molecular release in both types of hydrogels, and then, we discuss the impact of the gelation reaction. We will first describe continuous and discontinuous bulk rheological measurements in the PEG–norbornene hydrogel and then compare these results to the same measurements in the PEG–maleimide hydrogel. After determining the effect of shear on degradation and release, we then correlate molecular release with enzymatic degradation during continuous and minimal shear. We correlate evolution of the normalized storage moduli with the mass release percentage of molecules in PEG–norbornene and PEG–maleimide hydrogels and describe differences between these two materials. Then, the evolution of normalized storage moduli is correlated with the change in normalized gel intensity and normalized gel volume in release experiments.

Continuous and discontinuous bulk measurements of radical-initiated photopolymerized PEG–norbornene hydrogels are shown in Figure 1a. The storage moduli are plotted as a function of degradation time. In PEG–norbornene hydrogels, the crosslinking reaction only occurs in the presence of UV light. Without UV light exposure, no additional crosslinks

can be formed. Therefore, in PEG–norbornene hydrogels, we test the hypothesis that shear added to the material causes an increase in the scaffold modulus. In Figure 1a, the storage moduli continuously decrease as a function of time until a lower plateau is reached. This trend is measured in all samples and is independent of the measurement method used. Additionally, G' values measured for continuous and discontinuous bulk rheological measurements are within error of each other. This result suggests that shear has no effect on the rheological evolution of the photopolymerized hydrogel scaffold during enzymatic degradation. It also indicates that shear does not induce structural changes that would result in an increase in moduli in the scaffold during degradation.

Rheological characterization of enzymatic degradation of the base-initiated crosslinking PEG–maleimide hydrogel is shown in Figure 1b. Continuous bulk degradation measurements show that G' begins at around 600 Pa at $t = 0$ min. As the hydrogel is incubated longer, the value of G' increases for the first 40 min. At 40 min, G' is approximately 1200 Pa and reaches a maximum. Then, the value decreases until complete degradation. This increase in the modulus is similar to that reported in the literature in a comparable PEG-based hydrogel system.¹⁸ For the base-initiated PEG–maleimide hydrogel, this could be due to either shear or the crosslinking reaction. To determine the role of shear, we compare continuous and discontinuous rheological measurements. Each measurement of G' is within error regardless of the measurement technique. This result indicates that shear is not the reason we measure an increase in the modulus after degradation initiation.

The second possible cause could be the crosslinking reaction. This hydrogel can spontaneously form crosslinks between unreacted functional groups. We hypothesize that during swelling, unreacted functional groups are able to find complimentary chemistries and react to increase the elastic modulus of the gel. There are several mechanisms that can enable further crosslinking. After degradation initiation by incubation in enzymes, 4-arm polymers and 2-arm crosslinkers that are not crosslinked in the network can diffuse through the porous scaffold and out of the structure. This would result in a decrease in the modulus, if this was the dominant mechanism. During diffusion, these molecules can also react and attach to the network. In addition, partially crosslinked polymers with unreacted arms can react further with available partially reacted crosslinkers or unattached crosslinkers that are diffusing out of the scaffold. These are potential mechanisms that could cause the gel to crosslink further.

To support our hypothesis, we calculate the gel point and the probability that the 4-arm PEG molecule will have an unreacted functional group at the gel point. In our system, the crosslinking reaction occurs between 4-arm polymers and crosslinkers with two functional groups. Using Flory–Stock-mayer theory, we calculate the critical fraction of PEG functional sites needed to form a gel, p_c , using $p_c = \frac{1}{\sqrt{(f_B - 1)(f_A - 1) / r}}$, where $f_B = 2$, which is the functionality of the crosslinker, and $f_A = 4$, which is the functionality of the polymer backbone. $r = \frac{f_B n_B}{f_A n_A}$ is the stoichiometric ratio of the crosslinker to the backbone, where n_A represents the moles of the polymer backbone and n_B represents the moles of the crosslinker. We calculate $p_c = 0.46$ for PEG–norbornene gels and $p_c = 0.63$ for

PEG–maleimide gels. From these calculations, there will be functional groups on the PEG molecules in both gels that will be available for additional crosslinking.

We then calculate the probability of a 4-arm star PEG molecule having a single unreacted functional group at the gel point. We do this calculation using the critical fraction of PEG functional sites needed to form a gel, p_c , calculated from Flory–Stockmayer theory. This is the minimal fraction of PEG functional groups that need to be reacted to form a gel. Since we calculate this at the gel point, there will be additional crosslinks that form as the gel equilibrates, and this probability will decrease but does indicate that there are unreacted functional groups when the material has formed a gel. We calculate $P(F_{\text{PEG}}^{\text{out}})$, which is the probability that a reactive site results in a finite chain, which would remain unreacted or would not continue network growth.⁵⁸ $P(F_{\text{PEG}}^{\text{out}})$ is calculated using

$$P(F_{\text{PEG}}^{\text{out}}) = \left(\frac{1}{p_c} - 0.75 \right)^{0.5} - 0.5. \quad (3)$$

We determine $P(F_{\text{PEG}}^{\text{out}}) = 0.69$ for PEG–norbornene hydrogels and $P(F_{\text{PEG}}^{\text{out}}) = 0.41$ for PEG–maleimide hydrogels. There is a large probability in both materials at the gel point that there will be at least one functional group that has not reacted and will be available to form further crosslinks.

For PEG–norbornene gels, there are unreacted functional groups, but due to the chemistry, these can only react further when the material is exposed to UV light. Therefore, we do not measure an increase in the modulus when the material is incubated. For PEG–maleimide gels, there is also a high probability that there will be functional groups available to make a crosslink. The PEG–maleimide gel can crosslink further during incubation. As the material is incubated, molecule arms with functional groups can start to move and react. The degradation reaction also enhances the transport of molecules through the network. As degradation proceeds, more crosslinks break, providing more space and freedom for the materials to transport through the porous scaffold, where unreacted functional groups can meet and react. The rheology of our base-initiated crosslinked hydrogel has both additional crosslinking and scaffold degradation. The crosslinking reaction is dominant when G' increases, and degradation is dominant when G' decreases. Together, the significant difference in evolution of the storage modulus between our radical-initiated photopolymerized and base-initiated polymerized hydrogel shows that the crosslinking reaction plays an important role in rheological evolution during scaffold degradation, which indicates that it will also change molecular release.

Additionally, the calculations that we have provided assume that network growth is ideal. Flory–Stockmayer theory assumes that (1) all of the same functional groups are equally reactive, (2) all groups react independently, and (3) there are no intramolecular reactions.^{58–62} This assumes a very idealized network, which is likely not an accurate description of either of the scaffolds characterized in this work. In addition, the work by Miller and Macosko also assumes the same ideal network assumptions of Flory and Stockmayer.⁵⁸ Although our networks are not ideal, these calculations indicate that we will

not have 100% reaction of functional groups. This supports our hypothesis that there will be remaining functional groups in the PEG–maleimide networks that can react when the material is incubated in collagenase.

The effect of shear on molecular release is also characterized. These experiments measure the release profile from materials under constant shaking (defined as shake release) and without shaking (defined as nonshake release). The results of these experiments for both scaffolds are shown in Figure 2. The release profile is the cumulative mass release percentage as a function of time described by eq 2. Figure 2a compares the release profiles of radical-initiated photopolymerized PEG–norbornene hydrogels under both experimental conditions. All measurements have a similar release profile with the release percentage steadily increasing until it reaches a plateau. This is measured regardless of the conditions during material incubation, either constant or no shaking. Although the trend in release is the same regardless of incubation conditions, the hydrogels that undergo constant shaking do release molecules on a shorter time scale. The time to reach 100% release for the gels that are constantly shook is about 60 min shorter than for the gels that are not shook. Therefore, shaking a material does facilitate molecular release. When the release percentage is plotted against normalized time $t_{norm} = \frac{t}{t_{max}}$, where t_{max} is the time at the end of release measurements), the release percentage is within error of each other at each data point regardless of experimental conditions, as shown in Figure S6 in the Supporting Information. This again indicates that shear has no obvious effect on the release mechanism for radical-initiated crosslinking hydrogels.

Statistical analysis of all three replicates for each experimental condition for molecular release from PEG–norbornene is done. The time for 100% release is $t_{shake} = 169 \pm 44$ min and $t_{non-shake} = 214 \pm 14$ min for constant and no shaking conditions, respectively. These values are within error. An F -test and t -test show that the time for 100% release is statistically insignificant using the threshold $p < 0.05$. This confirms that shear does not change molecular release in radical-initiated photopolymerized hydrogel scaffolds.

Figure 2b shows the release profile from the base-initiated crosslinking PEG–maleimide hydrogel scaffold. PEG–maleimide has slow initial release with around 20% released in 50 min, followed by increased release up to 130 min of incubation and then sustained release for the remaining time. In PEG–maleimide, the release profiles are the same regardless of incubation conditions, which indicates that there is no effect of shear on molecular release from this scaffold. Similarly, an F -test and t -test show the time for 100% release is not statistically significant. $t_{shake} = 198 \pm 5$ min and $t_{non-shake} = 202 \pm 27$ min for the constant and no shaking incubation conditions, respectively. This indicates that shear does not facilitate drug release from the base-initiated polymerized hydrogel scaffold.

Molecular release from both PEG–norbornene and PEG–maleimide hydrogels is shown in Figure 2. Figure 2a shows molecular release from PEG–norbornene hydrogels, which shows relatively fast initial release (around 40%) in the first 50 min followed by sustained release until 200 min. In contrast, Figure 2b shows that there is slow initial release from PEG–maleimide hydrogels (approximately 20%) in the first 50 min followed by a gradual

increase in the percentage of released molecules. To further compare the difference in release profiles, all three replicates in sheared and nonsheared release experiments are fit with the Korsmeyer–Peppas–Ritger equation⁶³ to determine the release mechanism and release kinetic constant. The Korsmeyer–Peppas–Ritger model equation is

$$\frac{M_t}{M_\infty} = kt^n \quad (4)$$

where M_t is the cumulative mass released over time t , M_∞ is the total mass released throughout the experiment, n is the release exponent, which indicates the molecular release mechanism, and k is the release kinetic constant. It should be noted that data up to 60% release are used to fit this equation because this is the regime where the model is valid. All the calculated values from this fitting are listed in Table 1. Statistical analysis shows that the release exponents are statistically significant ($p < 0.05$) between the two types of crosslinking reactions. This indicates that the type of crosslinking reaction changes the molecule release mechanism. In radical-initiated PEG–norbornene hydrogels, we measure a zero-order release profile with a release exponent (n) approximately equal to 1. This indicates that release is driven by enzymatic degradation, as shown in Figure S9a,b in the Supporting Information. For base-initiated PEG–maleimide hydrogels, we measure a super case II release profile with a release exponent $n > 1$, as shown in Figure S9c,d. At the beginning of degradation, additional crosslinking reactions slow release, which causes $n > 1$. After additional crosslinking ends, degradation becomes the dominant reaction, and release is correlated with enzymatic degradation. For both hydrogels, shear has no effect on molecular release. Therefore, the role of shear in both enzymatic degradation and molecular release for either of the scaffolds is minimal. Since shear does not change degradation or release, we establish a quantitative correlation of release with rheological evolution during degradation.

The relationship between molecular release and enzymatic degradation is first characterized when materials undergo continuous shear or constant shaking. These conditions both impart shear on the material and should increase transport. For the radical-initiated photopolymerized PEG–norbornene hydrogels, the relation between molecular release and rheology during degradation is shown in Figure 3a. In this figure, we plot the unreleased percentage of fluorescent molecules from the gel ($Unreleased \% = \left(1 - \frac{M_t}{M_\infty}\right) \times 100\%$) on the left y axis and the normalized storage modulus of the gels $G'_{norm} = \frac{G' - G'_{min}}{G'_{max} - G'_{min}}$, where G'_{max} and G'_{min} are the maximum and minimum value of storage moduli of the material during degradation) on the right y axis. $Unreleased \%$ and G'_{norm} are plotted as a function of normalized time $t_{norm} = \frac{t}{t_{max}}$. The unreleased mass percentage decreases as the normalized storage modulus decreases. These two measurements are directly related over the entire degradation reaction. This indicates that molecular release from the PEG–norbornene hydrogel is driven by enzymatic degradation.

Figure 3b shows the unreleased mass percentage of fluorescent molecules and normalized modulus measurements over normalized time for the base-initiated PEG–maleimide

hydrogel. Initially, the unreleased percentage decreases slightly, $\approx 10\%$, as the normalized modulus percentage increases. This is the part of the reaction where additional crosslinking is occurring. Only a small amount of release happens because the gel is forming more crosslinks. More significant release occurs after G'_{norm} passes the maximum value, and degradation becomes the dominant reaction. After this point, the *Unreleased %* and G'_{norm} are within error of each other and follow the same trend. These results suggest that the release of tethered molecules from PEG–maleimide hydrogels is driven by both network crosslinking and enzymatic degradation. We also determine that the *Unreleased %* is directly correlated with G'_{norm} when degradation dominates.

This quantitative correlation of the unreleased mass percentage of PEG–fluorescein and normalized storage moduli is further analyzed by plotting these variables against each other and fitting the data using a linear fit, Figure S8 in the Supporting Information. It should be noted that since all points are not taken at the same time during the degradation reaction, the time is approximated to plot these measurements together. A linear correlation is fit using all data points for the PEG–norbornene hydrogels. For the PEG–maleimide hydrogels, only data when degradation is dominant are fit. An example dataset for a PEG–maleimide hydrogel is provided in Table S1 in the Supporting Information. We determine that the correlation (slope) is statistically insignificant ($p > 0.05$) for the same scaffold incubated with constant or minimal shear. In Table S2, PEG–norbornene hydrogels have a slope of 99.92 ± 6.78 under shear and a slope of 94.75 ± 4.37 under minimal shear. For PEG–maleimide hydrogels, the slope is 86.11 ± 7.31 under shear, and the slope is 88.78 ± 5.18 under minimal shear. These results indicate that shear has no effect on the correlation of molecular release with scaffold degradation. In addition, the fit of the correlation for PEG–norbornene hydrogels is statistically significant ($p < 0.05$) when compared to that for PEG–maleimide hydrogels. This result indicates that the type of crosslinking reaction does change the correlation between molecular release and rheological evolution during degradation.

We also measure the normalized gel intensity $I_{\text{norm}} = \frac{I - I_{\text{min}}}{I_{\text{max}} - I_{\text{min}}}$, where I is the gel intensity and I_{max} and I_{min} are the measured maximum and minimum gel intensity, respectively) and normalized gel volume $V_{\text{norm}} = \frac{V - V_{\text{min}}}{V_{\text{max}} - V_{\text{min}}}$, where V is the gel volume, V_{max} is the volume measured at $t = 0$ min prior to incubation in the enzyme solution, and V_{min} is the volume measured at the end of scaffold degradation) and correlate these variables with the normalized storage modulus $G'_{\text{norm}} = \frac{G' - G'_{\text{min}}}{G'_{\text{max}} - G'_{\text{min}}}$. Figure 4a shows this relationship for radical-initiated photopolymerized PEG–norbornene hydrogels. The gel intensity decreases as G'_{norm} decreases until they reach a plateau. Since the photopolymerized gel cannot form additional crosslinks without additional UV light exposure, molecular release from this scaffold is only facilitated by enzymatic degradation. This constant degradation is also measured by measuring the change in the volume of the hydrogel scaffold. The hydrogel volume decreases as G'_{norm} decreases throughout the degradation reaction. This result further confirms that molecular release from this photopolymerized hydrogel is driven by enzymatic degradation.

The same measurements are taken for the base-initiated PEG–maleimide hydrogel and are shown in Figure 4b. After incubation is begun, the gel intensity increases as the moduli increase. After the maximum modulus and gel intensity are measured, both quantities decrease until the material is degraded. The increase in gel intensity is unexpected because no additional fluorescent molecules are added to the scaffold during the experiment. We would expect that there would be no change in gel intensity even if the material crosslinks further. To explain this change in gel fluorescence, we also measure the change in the volume of the hydrogel during release. The volume of the hydrogel decreases over time including when the crosslinking reaction is dominant and minimal release is measured. Taken together, this means that the gel shrinks due to the additional crosslinks formed, and minimal molecules are released from the scaffold. Therefore, there is a similar amount of fluorescent molecules in a smaller volume of gel, which increases the PEG–fluorescein concentration and gel intensity. This relation also confirms that molecular release from the PEG–maleimide hydrogel is determined by both the crosslinking reaction and enzymatic degradation.

To correlate molecular release with bulk rheology during degradation for scaffolds under minimal shear, we compare two parallel experiments: (1) discontinuous bulk degradation and (2) molecular release when samples are not shook. Figure 5 shows the unreleased percentage of fluorescent molecules and the normalized modulus for materials incubated under these conditions. We measure a decrease in the unreleased percentage of PEG–fluorescein as G'_{norm} decreases with time in both hydrogel scaffolds. For the photopolymerized PEG–norbornene hydrogel, G'_{norm} and *Unreleased %* have a direct correlation over the measured time, with both variables decreasing until they reach a plateau at 0. This is the same relationship measured when this material is incubated with continuous shear, Figure 3a. There is more scatter in G'_{norm} measurements for early discontinuous bulk measurements. This is because each measurement is taken in a different gel. Even though there are larger errors in these measurements, data for both incubation conditions follow the same trend, and most points are within error. Together, we determine that shear has no effect on the correlation between degradation and molecular release.

The correlation for molecular release and degradation for base-initiated PEG–maleimide hydrogels is shown in Figure 5b. Molecular release is low as G'_{norm} increases; this is when the crosslinking reaction is dominant. More significant release is measured when G'_{norm} decreases, which is when scaffold degradation becomes dominant. *Unreleased %* of PEG–fluorescein molecules and G'_{norm} are directly correlated after reaching the maximum value of G'_{norm} , which is the same phenomenon measured in Figure 3b. This correlation indicates that the release of tethered molecules from our base-initiated crosslinking hydrogel is first minimal due to increased crosslinking and is indirectly correlated with the modulus. Once the modulus reaches a maximum and starts to decrease, material degradation dominates, and molecular release and rheological evolution are indirectly correlated. In summary, the same correlation between molecular release and rheological evolution is measured regardless of the incubation conditions, indicating that shear does not change these processes.

The correlation of gel intensity, gel volume, and rheological evolution is also measured when both scaffolds are incubated with minimal shear. In PEG–norbornene hydrogels shown

in Figure S7a in the Supporting Information, the normalized gel intensity (I_{norm}) and normalized gel volume (V_{norm}) decrease as normalized storage moduli (G'_{norm}) decrease until they reach a plateau at 0. These correlations are the same as those measured when the material is incubated with shear in Figure 4a. The base-initiated polymerized PEG–maleimide hydrogel also has similar results as gels incubated with constant shear. In minimal shear, gel intensity increases as G'_{norm} increases, and the gel volume decreases, as shown in Figure S7b in the Supporting Information. This is the same trend measured when incubated with constant shear. Comparing with Figure 4b, we determine a similar correlation between molecular release and scaffold degradation for this material under minimal shear.

CONCLUSIONS

In this work, we build quantitative correlations between molecular release and scaffold degradation. Two types of enzymatically degradable PEG–peptide hydrogels are characterized—a radical-initiated photopolymerized hydrogel (PEG–norbornene) and a base-initiated polymerized hydrogel (PEG–maleimide). These two materials gel through step-growth crosslinking reactions. Both scaffolds have the same degradable crosslinker, which enables them to be degraded by the same enzymatic degradation reaction. To correlate bulk rheological properties with molecular release, we tether PEG–fluorescein into our network and characterize the rheological evolution and molecular release from both scaffolds.

Previous work measured an increase in the modulus during degradation in enzyme crosslinked hydrogels.¹⁸ They hypothesized that shear imparted on the scaffold during rheological characterization caused a change in the network connectivity and structure. We tested this hypothesis by characterizing both scaffolds during enzymatic degradation under continuous and minimal shear during bulk rheological characterization and molecular release. Bulk rheological and molecular release measurements show that after initiation of degradation, the radical-initiated PEG–norbornene hydrogel moduli consistently decrease, and the amount of fluorescent molecules released consistently increases. The material moduli are indirectly correlated with the percentage of released fluorescent molecules. These results do not change when the hydrogel is incubated with constant or minimal shear. For the base-initiated PEG–maleimide hydrogel, we measure an increase in moduli after we begin incubating the material with enzymes. This increase also corresponds to minimal release of fluorescent molecules from the scaffold, an increase in the gel intensity, and a decrease in the gel volume. This change in gel intensity is due to an increase in fluorescent molecule concentration in the gel because the crosslinking reaction decreases the gel volume. After the maximum modulus is measured, the material then degrades with consistent decreases in moduli and increases in molecular release. The material moduli are indirectly correlated to the percentage of released fluorescent molecules from the scaffold when degradation is dominant. All results are independent of shear imparted during scaffold incubation. Together, these results show that the type of crosslinking reaction changes both material degradation and molecular release and should be considered during design of drug delivery vehicles.

Correlating rheology with molecular release is important especially in drug delivery vehicles that are designed to release molecules as they degrade. We determine that the storage modulus is quantitatively correlated with release performance in these biodegradable materials. This work provides a new method to measure and predict drug release using material rheology and can inform material design and engineering of targeted drug delivery vehicles.

Supplementary Material

Refer to Web version on PubMed Central for supplementary material.

ACKNOWLEDGMENTS

The authors acknowledge Prof. Simon A. Rogers from the University of Illinois at Urbana-Champaign for helpful discussions. Research reported in this publication was supported in part by the National Institute of General Medical Sciences of the National Institutes of Health under award number R15GM119065. The content is solely the responsibility of the authors and does not necessarily represent the official views of the National Institutes of Health.

REFERENCES

- (1). Ashley GW; Henise J; Reid R; Santi DV Hydrogel drug delivery system with predictable and tunable drug release and degradation rates. *Proc. Natl. Acad. Sci. U.S.A* 2013, 110, 2318–2323. [PubMed: 23345437]
- (2). Fu Y; Kao WJ Drug release kinetics and transport mechanisms of non-degradable and degradable polymeric delivery systems. *Expet Opin. Drug Deliv* 2010, 7, 429–444.
- (3). Kamaly N; Yameen B; Wu J; Farokhzad OC Degradable Controlled-Release Polymers and Polymeric Nanoparticles: Mechanisms of Controlling Drug Release. *Chem. Rev* 2016, 116, 2602–2663. [PubMed: 26854975]
- (4). Shih H; Lin C-C Cross-Linking and Degradation of Step-Growth Hydrogels Formed by Thiol-Ene Photoclick Chemistry. *Biomacromolecules* 2012, 13, 2003–2012. [PubMed: 22708824]
- (5). Aimetti AA; Machen AJ; Anseth KS Poly(ethylene glycol) hydrogels formed by thiol-ene photopolymerization for enzyme-responsive protein delivery. *Biomaterials* 2009, 30, 6048–6054. [PubMed: 19674784]
- (6). Lee KY; Bouhadir KH; Mooney DJ Controlled degradation of hydrogels using multi-functional cross-linking molecules. *Biomaterials* 2004, 25, 2461–2466. [PubMed: 14751730]
- (7). Zustiak SP; Leach JB Hydrolytically Degradable Poly(Ethylene Glycol) Hydrogel Scaffolds with Tunable Degradation and Mechanical Properties. *Biomacromolecules* 2010, 11, 1348–1357. [PubMed: 20355705]
- (8). Madl CM; Katz LM; Heilshorn SC Tuning Bulk Hydrogel Degradation by Simultaneous Control of Proteolytic Cleavage Kinetics and Hydrogel Network Architecture. *ACS Macro Lett.* 2018, 7, 1302–1307. [PubMed: 32523799]
- (9). Wang Y; Pisapati AV; Zhang XF; Cheng X Recent Developments in Nanomaterial-Based Shear-Sensitive Drug Delivery Systems. *Adv. Healthcare Mater* 2021, 10, 2002196.
- (10). Secret E; Kelly SJ; Crannell KE; Andrew JS Enzyme-Responsive Hydrogel Microparticles for Pulmonary Drug Delivery. *ACS Appl. Mater. Interfaces* 2014, 6, 10313–10321. [PubMed: 24926532]
- (11). Washington MA; Swiner DJ; Bell KR; Fedorchak MV; Little SR; Meyer TY The impact of monomer sequence and stereochemistry on the swelling and erosion of biodegradable poly(lactic-co-glycolic acid) matrices. *Biomaterials* 2017, 117, 66–76. [PubMed: 27936418]
- (12). Schultz KM; Anseth KS Monitoring degradation of matrix metalloproteinases-cleavable PEG hydrogels via multiple particle tracking microrheology. *Soft Matter* 2013, 9, 1570–1579.

- (13). Wehrman MD; Lindberg S; Schultz KM Quantifying the dynamic transition of hydrogenated castor oil gels measured via multiple particle tracking microrheology. *Soft Matter* 2016, 12, 6463–6472. [PubMed: 27396611]
- (14). Daviran M; Caram HS; Schultz KM Role of cell-mediated enzymatic degradation and cytoskeletal tension on dynamic changes in the rheology of the pericellular region prior to human mesenchymal stem cell motility. *ACS Biomater. Sci. Eng* 2018, 4, 468–472. [PubMed: 29862316]
- (15). Escobar F; Anseth KS; Schultz KM Dynamic Changes in Material Properties and Degradation of Poly(ethylene glycol)-Hydrazone Gels as a Function of pH. *Macromolecules* 2017, 50, 7351–7360.
- (16). Joyner K; Yang S; Duncan GA Microrheology for biomaterial design. *APL Bioeng.* 2020, 4, 041508. [PubMed: 33415310]
- (17). Mazzeo MS; Chai T; Daviran M; Schultz KM Characterization of the Kinetics and Mechanism of Degradation of Human Mesenchymal Stem Cell-Laden Poly(ethylene glycol) Hydrogels. *ACS Appl. Bio Mater* 2018, 2, 81–92.
- (18). Sun Han Chang R; Lee JC-W; Pedron S; Harley BAC; Rogers SA Rheological analysis of the gelation kinetics of an enzyme cross-linked PEG hydrogel. *Biomacromolecules* 2019, 20, 2198–2206. [PubMed: 31046247]
- (19). Meyvis T; De Smedt S; Stubbe B; Hennink W; Demeester J On the release of proteins from degrading dextran methacrylate hydrogels and the correlation with the rheologic properties of the hydrogels. *Pharm. Res* 2001, 18, 1593–1599. [PubMed: 11758768]
- (20). Thapa K Thiol-induced degradation of hydrogels utilizing multiresponsive dithioma- leimides crosslinkers. Honors Thesis; The University of Southern Mississippi, 2020.
- (21). Schultz KM; Baldwin AD; Kiick KL; Furst EM Measuring the modulus and reverse percolation transition of a degrading hydrogel. *ACS Macro Lett.* 2012, 1, 706–708. [PubMed: 23413411]
- (22). Wehrman MD; Lindberg S; Schultz KM Impact of shear on the structure and rheological properties of a hydrogenated castor oil colloidal gel during dynamic phase transitions. *J. Rheol* 2018, 62, 437–446.
- (23). Wu N; Schultz KM Microrheological characterization of covalent adaptable hydrogel degradation in response to temporal pH changes that mimic the gastrointestinal tract. *Soft Matter* 2020, 16, 6253–6258. [PubMed: 32500893]
- (24). Wu N; Schultz KM Microrheological characterization of covalent adaptable hydrogels for applications in oral delivery. *Soft Matter* 2019, 15, 5921–5932. [PubMed: 31282533]
- (25). Ulijn RV; Bibi N; Jayawarna V; Thornton PD; Todd SJ; Mart RJ; Smith AM; Gough JE Bioresponsive hydrogels. *Mater. Today* 2007, 10, 40–48.
- (26). Kost J; Leong K; Langer R Ultrasound-enhanced polymer degradation and release of incorporated substances. *Proc. Natl. Acad. Sci. U.S.A* 1989, 86, 7663–7666. [PubMed: 2813349]
- (27). Kost J Ultrasound-Triggered Delivery of Peptides and Proteins from Microspheres. *Microparticulate Systems for the Delivery of Proteins and Vaccines*; CRC Press, 2020; pp 463–476.
- (28). Kubota T; Kurashina Y; Zhao J; Ando K; Onoe H Ultrasound-triggered on-demand drug delivery using hydrogel microbeads with release enhancer. *Mater. Des* 2021, 203, 109580.
- (29). Liu L; Zhang Y; Yu S; Zhang Z; He C; Chen X pH- and Amylase-Responsive Carboxymethyl Starch/Poly(2-isobutyl-acrylic acid) Hybrid Microgels as Effective Enteric Carriers for Oral Insulin Delivery. *Biomacromolecules* 2018, 19, 2123–2136. [PubMed: 29664632]
- (30). Wang S; Attah R; Li J; Chen Y; Chen R A pH-Responsive Amphiphilic Hydrogel Based on Pseudopeptides and Poly(ethylene glycol) for Oral Delivery of Hydrophobic Drugs. *ACS Biomater. Sci. Eng* 2018, 4, 4236–4243. [PubMed: 33418822]
- (31). Schwoerer ADA; Harling S; Scheibe K; Menzel H; Daniels R Influence of degree of substitution of HES-HEMA on the release of incorporated drug models from corresponding hydrogels. *Eur. J. Pharm. Biopharm* 2009, 73, 351–356. [PubMed: 19683570]
- (32). Branco MC; Pochan DJ; Wagner NJ; Schneider JP Macromolecular diffusion and release from self-assembled β -hairpin peptide hydrogels. *Biomaterials* 2009, 30, 1339–1347. [PubMed: 19100615]

- (33). Cinay GE; Erkoç P; Alipour M; Hashimoto Y; Sasaki Y; Akiyoshi K; Kizilel S Nanogel-integrated pH-responsive composite hydrogels for controlled drug delivery. *ACS Biomater. Sci. Eng* 2017, 3, 370–380. [PubMed: 33465934]
- (34). Kim AR; Lee SL; Park SN Properties and in vitro drug release of pH- and temperature-sensitive double cross-linked interpenetrating polymer network hydrogels based on hyaluronic acid/poly (N-isopropylacrylamide) for transdermal delivery of luteolin. *Int. J. Biol. Macromol* 2018, 118, 731–740. [PubMed: 29940230]
- (35). Santoveña A; Alvarez-Lorenzo C; Concheiro A; Llabres M; Farina J Rheological properties of PLGA film-based implants: correlation with polymer degradation and SPf66 antimalaric synthetic peptide release. *Biomaterials* 2004, 25, 925–931. [PubMed: 14609681]
- (36). Lin C-C; Metters AT Hydrogels in controlled release formulations: network design and mathematical modeling. *Adv. Drug Delivery Rev* 2006, 58, 1379–1408.
- (37). Lao LL; Peppas NA; Boey FYC; Venkatraman SS Modeling of drug release from bulk-degrading polymers. *Int. J. Pharm* 2011, 418, 28–41. [PubMed: 21182912]
- (38). Peppas NA; Narasimhan B Mathematical models in drug delivery: How modeling has shaped the way we design new drug delivery systems. *J. Controlled Release* 2014, 190, 75–81.
- (39). Daviran M; Longwill SM; Casella JF; Schultz KM Rheological characterization of dynamic remodeling of the pericellular region by human mesenchymal stem cell-secreted enzymes in well-defined synthetic hydrogel scaffolds. *Soft Matter* 2018, 14, 3078–3089. [PubMed: 29667686]
- (40). Holmes R; Yang X-B; Dunne A; Florea L; Wood D; Tronci G Thiol-Ene Photo-Click Collagen-PEG Hydrogels: Impact of Water-Soluble Photoinitiators on Cell Viability, Gelation Kinetics and Rheological Properties. *Polymers* 2017, 9, 226.
- (41). Fairbanks BD; Schwartz MP; Halevi AE; Nuttelman CR; Bowman CN; Anseth KS A versatile synthetic extracellular matrix mimic via thiol-norbornene photopolymerization. *Adv. Mater* 2009, 21, 5005–5010. [PubMed: 25377720]
- (42). Wehrman MD; Leduc A; Callahan HE; Mazzeo MS; Schumm M; Schultz KM Rheological properties and structure of step- and chain-growth gels concentrated above the overlap concentration. *AIChE J.* 2018, 64, 3168–3176.
- (43). Jansen LE; Negrón-Piñero LJ; Galarza S; Peyton SR Control of thiol-maleimide reaction kinetics in PEG hydrogel networks. *Acta Biomater.* 2018, 70, 120–128. [PubMed: 29452274]
- (44). Fu Y; Kao WJ In situ forming poly(ethylene glycol)-based hydrogels via thiol-maleimide Michael-type addition. *J. Biomed. Mater. Res., Part A* 2011, 98A, 201–211.
- (45). Liu S; Cao H; Guo R; Li H; Lu C; Yang G; Nie J; Wang F; Dong N; Shi J; et al. Effects of the proportion of two different cross-linkers on the material and biological properties of enzymatically degradable PEG hydrogels. *Polym. Degrad. Stab* 2020, 172, 109067.
- (46). Paolino D; Tudose A; Celia C; Di Marzio L; Cilurzo F; Mircioiu C Mathematical models as tools to predict the release kinetic of fluorescein from lyotropic colloidal liquid crystals. *Materials* 2019, 12, 693.
- (47). Abulateefeh SR; Alkawareek MY; Alkilany AM Tunable sustained release drug delivery system based on mononuclear aqueous core-polymer shell microcapsules. *Int. J. Pharm* 2019, 558, 291–298. [PubMed: 30641178]
- (48). Liu Y; Miyoshi H; Nakamura M Novel drug delivery system of hollow mesoporous silica nanocapsules with thin shells: preparation and fluorescein isothiocyanate (FITC) release kinetics. *Colloids Surf., B* 2007, 58, 180–187.
- (49). Boehler C; Güder F; Küçükbayrak UM; Zacharias M; Asplund M A simple approach for molecular controlled release based on atomic layer deposition hybridized organic-inorganic layers. *Sci. Rep* 2016, 6, 19574. [PubMed: 26791399]
- (50). Ruskowitz ER; Comerford MP; Badeau BA; DeForest CA Logical stimuli-triggered delivery of small molecules from hydrogel biomaterials. *Biomater. Sci* 2019, 7, 542–546. [PubMed: 30556545]
- (51). Schoener CA; Hutson HN; Peppas NA pH-responsive hydrogels with dispersed hydrophobic nanoparticles for the delivery of hydrophobic therapeutic agents. *Polym. Int* 2012, 61, 874–879. [PubMed: 23087546]

- (52). Lin C-C; Anseth KS PEG hydrogels for the controlled release of biomolecules in regenerative medicine. *Pharm. Res* 2009, 26, 631–643. [PubMed: 19089601]
- (53). Park JD; Ahn KH; Wagner NJ Structure-rheology relationship for a homogeneous colloidal gel under shear startup. *J. Rheol* 2017, 61, 117–137.
- (54). Fairbanks BD; Schwartz MP; Bowman CN; Anseth KS Photoinitiated polymerization of PEG-diacrylate with lithium phenyl-2,4,6-trimethylbenzoylphosphinate: polymerization rate and cytocompatibility. *Biomaterials* 2009, 30, 6702–6707. [PubMed: 19783300]
- (55). Li L; Gu J; Zhang J; Xie Z; Lu Y; Shen L; Dong Q; Wang Y Injectable and biodegradable pH-responsive hydrogels for localized and sustained treatment of human fibrosarcoma. *ACS Appl. Mater. Interfaces* 2015, 7, 8033–8040. [PubMed: 25838258]
- (56). Cevik O; Gidon D; Kizilel S Visible-light-induced synthesis of pH-responsive composite hydrogels for controlled delivery of the anticonvulsant drug pregabalin. *Acta Biomater.* 2015, 11, 151–161. [PubMed: 25242648]
- (57). Qin Y; Wang X; Wang ZL Microfibre-nanowire hybrid structure for energy scavenging. *Nature* 2008, 451, 809–813. [PubMed: 18273015]
- (58). Miller DR; Macosko CW A New Derivation of Postgel Properties of Network Polymers. *Rubber Chem. Technol* 1976, 49, 1219–1231.
- (59). Flory PJ *Principles of Polymer Chemistry*; Cornell University Press, 1953.
- (60). Flory PJ Molecular size distribution in three dimensional polymers. II. Trifunctional branching units. *J. Am. Chem. Soc* 1941, 63, 3091–3096.
- (61). Flory PJ Molecular Size Distribution in Three Dimensional Polymers. III. Tetrafunctional Branching Units. *J. Am. Chem. Soc* 1941, 63, 3096–3100.
- (62). Larson RG *The Structure and Rheology of Complex Fluids*; Oxford university press: New York, 1999.
- (63). Ritger PL; Peppas NA A simple equation for description of solute release II. Fickian and anomalous release from swellable devices. *J. Controlled Release* 1987, 5, 37–42.

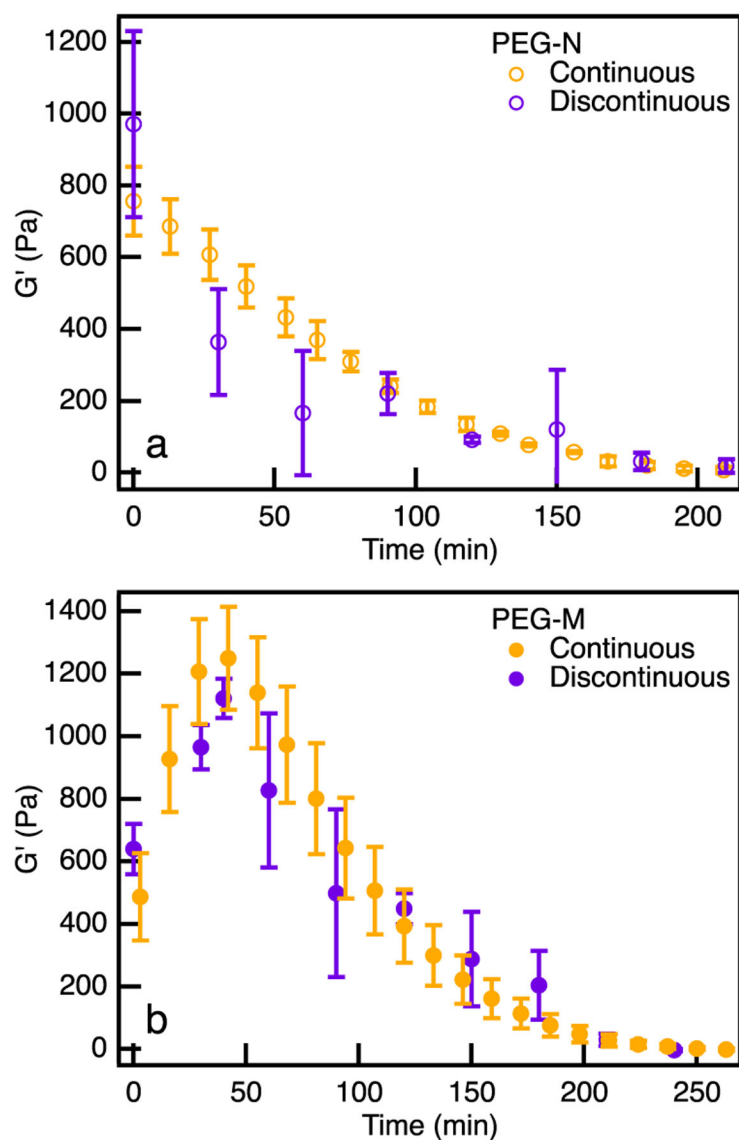


Figure 1. Enzymatic degradation measured using bulk rheology. The degradation reaction is initiated by immersion of a gel in 1 mg mL^{-1} collagenase solution. Bulk rheology measures the elastic moduli, G' , as a function of time of (a) radical-initiated photopolymerized PEG–norbornene (PEG–N) hydrogels and (b) base-initiated polymerized PEG–maleimide (PEG–M) hydrogels.

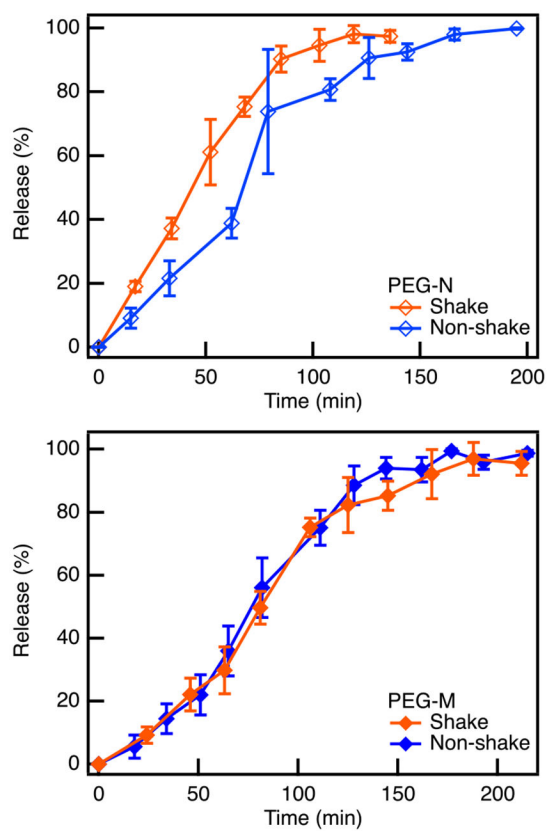


Figure 2. Molecular release from (a) radical-initiated photopolymerized PEG–norbornene (PEG–N) hydrogels and (b) base-initiated PEG–maleimide (PEG–M) hydrogels incubated in 1 mg mL⁻¹ collagenase. The cumulative mass release percentage is plotted as a function of time.

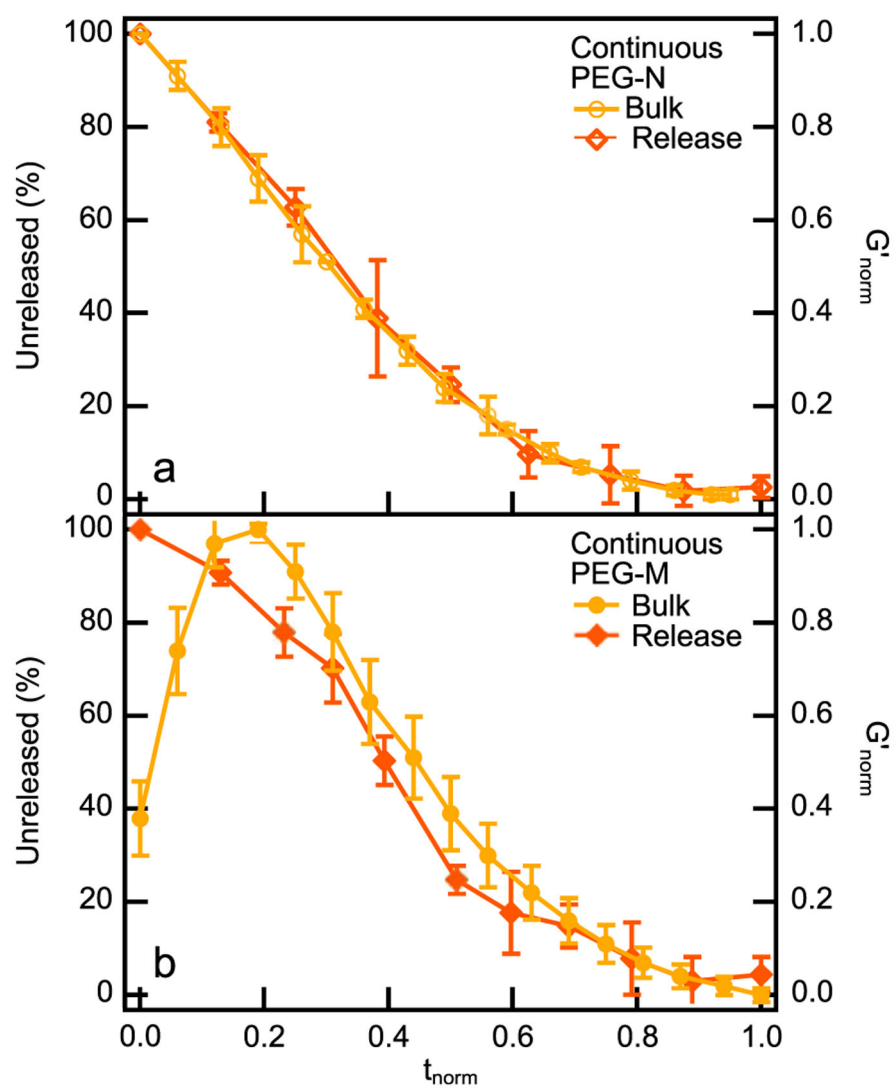


Figure 3. Unreleased mass percentage of the sol-sample and normalized storage moduli for (a) PEG–norbornene (PEG–N) and (b) PEG–maleimide (PEG–M) hydrogels under continuous shear or constant shaking.

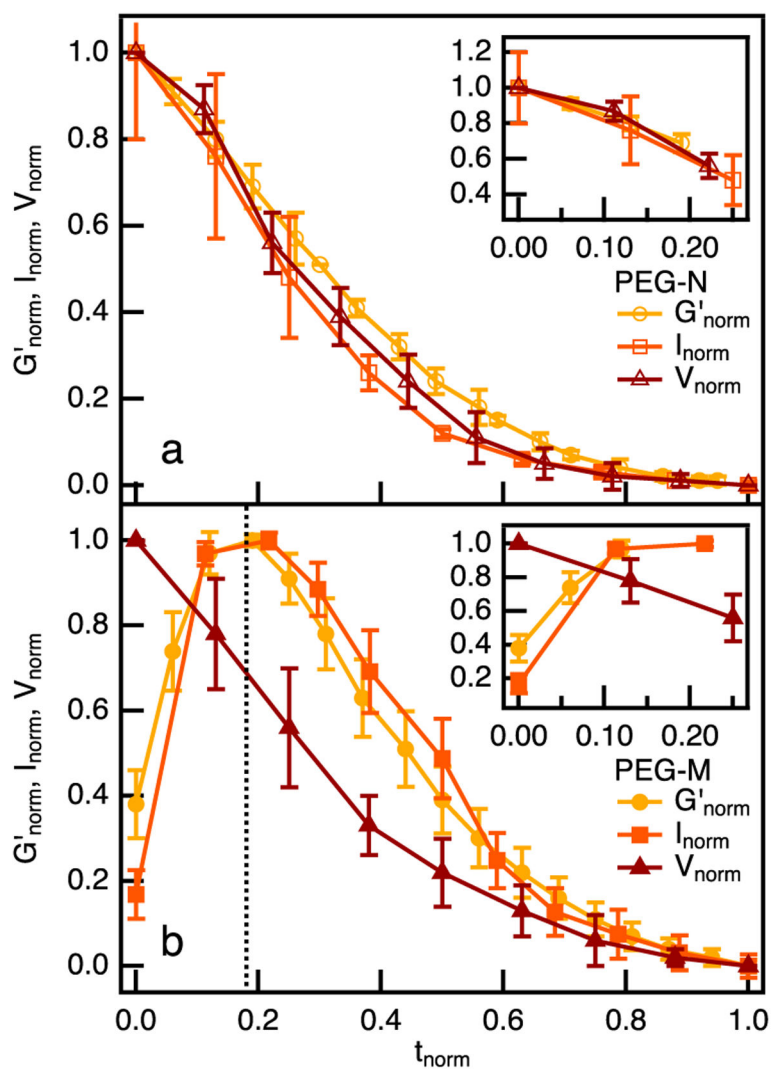


Figure 4. Normalized storage moduli (G'_{norm}), normalized gel intensity (I_{norm}), and normalized gel volume (V_{norm}) are plotted as a function of normalized time (t_{norm}) for (a) PEG–norbornene (PEG–N) and (b) PEG–maleimide (PEG–M) hydrogels under constant shear. The dash vertical line in (b) indicates where the value of G'_{norm} reaches a maximum.

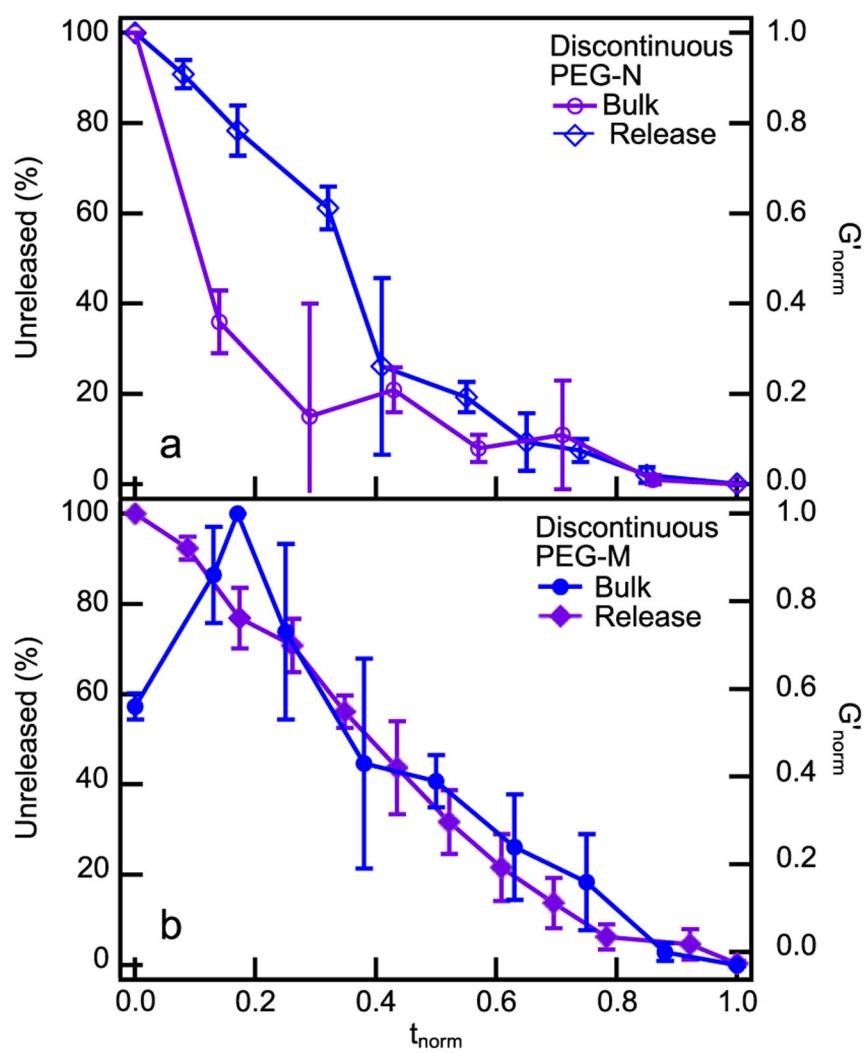


Figure 5. Cumulative percentage of unreleased PEG-fluorescein and normalized moduli for (a) PEG-norbornene (PEG-N) and (b) PEG-maleimide (PEG-M) hydrogels under minimal shear.

PEG-Fluorescein Release Kinetic Constant from Both Types of Hydrogels under Constant or Minimal Shear Obtained from Fitting Experimental Data Using eq 4^a

Table 1.

type of crosslinked hydrogel	shear		nonshear	
	k (min ⁻ⁿ)	n	k (min ⁻ⁿ)	n
radical-initiated photopolymerized PEG-norbornene hydrogel	0.0098 ± 0.0067	1.01 ± 0.22	0.0089 ± 0.0074	1.07 ± 0.44
base-initiated polymerized PEG-maleimide hydrogel	0.0005 ± 0.0006	1.64 ± 0.34	0.0012 ± 0.0018	1.56 ± 0.39

^a n is the release exponent, and k is the release kinetic constant.